NJC

PAPER

View Article Online
View Journal | View Issue



Cite this: *New J. Chem.*, 2017, 41, 12397

# A simple one-pot synthesis of a Zn(O,S)/$Ga_2O_3$ nanocomposite photocatalyst for hydrogen production and 4-nitrophenol reduction†

Hairus Abdullah, [ab] Noto Susanto Gultom [a] and Dong-Hau Kuo *[a]

Received 11th July 2017,
Accepted 31st August 2017

DOI: 10.1039/c7nj02505j

rsc.li/njc

Noble metal-free Zn(O,S)/$Ga_2O_3$ nanocomposite photocatalysts containing different amounts of $Ga_2O_3$ have been synthesized using a precipitation method at 90 °C. The as-prepared catalysts were characterized and their composite nature was confirmed. The Zn(O,S)/$Ga_2O_3$ catalysts were examined for their ability to evolve hydrogen under low UV light illumination (0.088 mW $cm^{-2}$) and to provide hydrogen for 4-nitrophenol (4-NP) reduction. Gas chromatography measurements revealed that hydrogen was produced at a rate of 280 μmol $g^{-1}$ $h^{-1}$ $W^{-1}$, while UV-vis absorption and high-performance liquid chromatography (HPLC) measurements confirmed the formation of 4-aminophenol (4-AP) as a product of 4-NP reduction. The heterojunction formation between the Zn(O,S) and $Ga_2O_3$ phases enhanced the photocatalytic activity, compared to the single Zn(O,S) and $Ga_2O_3$ phases. Surface oxygen anions and oxygen vacancies played important roles in the photocatalytic mechanism to evolve hydrogen and to utilize hydrogen ions in 4-NP reduction. The photocatalytic hydrogen evolution reaction and its utilization for 4-NP reduction to 4-AP were evaluated and elucidated in this work.

## 1 Introduction

Global warming is one of humanity's greatest concerns in the world today. Over the past few decades, many efforts have been devoted to searching for alternative renewable energy resources to reduce carbon emissions.[1–4] As one significant alternative, the utilization of hydrogen energy is very promising in overcoming global warming, due to its clean combustion product. Not only is hydrogen an energy carrier obtained using sunlight, but it can also be applied to the reduction of toxic 4-nitrophenol (4-NP), which is known as a stable toxic pollutant released from industries.[5] Furthermore, the reduced product of 4-NP, 4-aminophenol (4-AP), is useful for certain applications, such as the manufacture of dyes,[6] photographic developers,[7] and antipyretic drugs.[8] Most previous research has used $NaBH_4$ as a hydrogen source to reduce 4-NP in the presence of metal or metal oxide catalysts;[5,9,10] nevertheless, the excess $NaBH_4$ in solution is not desirable, due to its corrosive and irritative properties as stated in the material safety data sheet. It is possible to seek efficient catalysts for both hydrogen production and 4-NP reduction simultaneously, by utilizing a hydrogen evolution photocatalyst.

To evolve hydrogen from water, a photocatalyst commonly needs to satisfy some major requirements, such as a conduction band that is more negative than that of the water reduction potential,[11,12] a long lifetime of the photo-generated electrons and holes, and a large surface area, *etc.* Some semiconductor materials can fulfill only certain requirements but not all of them. Therefore, studies searching for photocatalyst materials that satisfy these requirements are needed to obtain better efficiency. Furthermore, photocatalysts with kinetically suitable electron transport from the photocatalyst surface to the water interface are required, so that energy losses due to charge transport and photo-carrier recombination can be minimized.[12] Some famous semiconductors such as ZnS, ZnO, $TiO_2$ and $Ga_2O_3$ have shown promising performances as hydrogen evolution catalysts in previous works.[13–16] These semiconductor materials exhibit a suitable energy band position for water reduction. Therefore, advanced research related to these materials is required to obtain highly efficient photocatalysts.

Several useful approaches to enhance the photocatalytic activity, such as solid solution formation,[17] heterojunction formation,[18,19] and surface and particle size modification[20,21] have been widely explored. Our previous work showed that Zn(O,S), formed from a solid solution of ZnS and ZnO, had significantly enhanced photocatalytic hydrogen evolution performance compared to the single oxide and sulfide phases under the same experimental conditions. It has been proposed that the formation of a solid solution creates some oxygen vacancy sites that are heavily involved in

[a] Department of Materials Science and Engineering, National Taiwan University of Science and Technology, No. 43, Sec. 4, Keelung Road, Taipei 10607, Taiwan. E-mail: dhkuo@mail.ntust.edu.tw; Fax: +886-2-27303291
[b] Department of Industrial Engineering, University of Prima Indonesia, Medan, Indonesia

† Electronic supplementary information (ESI) available. See DOI: 10.1039/c7nj02505j

the hydrogen evolution mechanism.[1] It has also been shown in our previous works[17–19] that heterojunction formation can significantly increase the photocatalytic activity. Furthermore, modifications made to the surface and particle size by utilizing larger $SiO_2$ spherical particles to increase adsorption and degradation of toxic organic dyes have been demonstrated in our previous works.[18]

The synergistic effect expected from the combination of a Zn(O,S) solid solution and a heterojunction, by forming a Zn(O,S)/$Ga_2O_3$ nanocomposite, is what motivated this work. In our previous work, the Zn(O,S) solid solution showed enhanced performance compared to the single phases of ZnO and ZnS. To achieve better photocatalytic activity, $Ga_2O_3$ was selected due to its suitable conduction band potential for water reduction.[12] After simultaneous photoexcitation of the Zn(O,S) and $Ga_2O_3$ nanoparticles, the excited electrons in the conduction band of one phase transfer to the other phase near the interface between them. As a result, this process increases the number of photo-generated electrons that promote photocatalytic activity on the catalyst surface.

In this work, the Zn(O,S)/$Ga_2O_3$ nanocomposite was synthesized in one pot using a simple precipitation method at 90 °C and normal pressure. The formation of $Ga_2O_3$ was easily achieved by adding a small amount of hydrazine monohydrate into thioacetamide solution at 90 °C. Different amounts of Ga precursor were used to obtain different amounts of $Ga_2O_3$ in the Zn(O,S)/$Ga_2O_3$ nanocomposites, in order to find a suitable composition to optimize the hydrogen evolution rate. The photocatalyst with the best performance was further utilized to reduce 4-NP to 4-AP without using any reducing agents. The relatively high hydrogen evolution rate and the ability of the photocatalyst to reduce 4-NP to 4-AP are presented, and an appropriate mechanism is elucidated in this paper.

## 2 Experimental section

### 2.1 Materials

All materials used in this work were commercially available and used without any further purification treatment.

### 2.2 Synthesis of Zn(O,S)/$Ga_2O_3$ nanocomposites

To synthesize Zn(O,S)/10% $Ga_2O_3$ nanocomposite powder, 4.4 g $Zn(Ac)_2{\cdot}2H_2O$ and 0.8 g $Ga(NO)_3{\cdot}8H_2O$ were first mixed in 500 mL deionized (DI) water under vigorous stirring. After all the precursors were totally dissolved, 0.75 g $C_2H_5NS$ as a sulfur source was added to the solution. The solution temperature was then increased to 90 °C and held for 4 h. The formation of a white precipitate was initiated in the solution at 70 °C. When the temperature reached 90 °C, 0.2 mL hydrazine monohydrate was added to the solution. The obtained white precipitate was naturally cooled down to room temperature and washed 3 times, followed by drying in a rotary evaporator. To completely eliminate all the volatile elements on the catalyst surfaces, the white powder was kept in a vacuum oven at 70 °C overnight. The obtained powder was denoted as the Zn(O,S)/10% $Ga_2O_3$ nanocomposite powder. The other Zn(O,S)/0.5% $Ga_2O_3$, Zn(O,S)/3% $Ga_2O_3$, Zn(O,S)/5% $Ga_2O_3$ and Zn(O,S)/20% $Ga_2O_3$ nanocomposite powders were also prepared with appropriate amounts of $Ga(NO)_3{\cdot}8H_2O$ using the same experimental procedure. Single phases of $Ga_2O_3$ and Zn(O,S) were also prepared with the same procedure without Zn and Ga precursors, respectively, for comparison.

### 2.3 Characterization

The morphology and microstructure of the Zn(O,S)/$Ga_2O_3$ nanocomposites were examined using field-emission scanning electron microscopy (FE-SEM, JSM 6500F, JEOL, Tokyo, Japan) and high-resolution transmission electron microscopy (HRTEM, Tecnai F20 G2, Philips, Netherlands). Powder X-ray diffraction (XRD) patterns of the Zn(O,S)/$Ga_2O_3$ nanocomposites with different amounts of Ga precursor were recorded on a Bruker D2-phaser diffractometer using Cu Kα radiation with a wavelength of 1.5418 Å. X-ray photoelectron spectroscopy (XPS) measurements of the Zn(O,S)/$Ga_2O_3$ nanocomposite powders were carried out on a VG ESCA Scientific Theta Probe spectrometer system with Al Kα (1486.6 eV) radiation and a 15–400 mm X-ray spot size, using an ion gun operated at 3 kV and 1 mA. The UV-vis diffuse reflectance spectra (DRS) of the Zn(O,S)/$Ga_2O_3$ nanocomposite powders were recorded using a Jasco V-670 UV-visible-near IR spectrophotometer. Mott–Schottky and electrochemical impedance spectroscopy (EIS) measurements of the Zn(O,S) and $Ga_2O_3$ powders were carried out using a Princeton Applied Research Versa STAT 3. A glassy carbon electrode, Ag/AgCl electrode and platinum wire were used as the working, reference and counter electrodes, respectively. For the EIS measurements, the window potential, frequency and scan rate values were set from −1.5 to 0.5 V, 5000–0.05 Hz and 0.05 V $s^{-1}$, respectively. The surface area of the as-prepared photocatalysts were finally investigated using the Brunauer–Emmett–Teller (BET) method.

### 2.4 Photocatalytic hydrogen evolution experiments

All the as-prepared nanocomposites were tested for their ability to produce hydrogen in a 500 mL reactor containing 10% ethanol solution under a 4 × 6 Watt UV blacklight tube lamp at a fixed wavelength of 352 nm for 5 h. The UV lamp illumination intensity was approximately 0.088 mW $cm^{-2}$ based on the photometer measurement. This intensity value is much lower than that of natural sunlight illumination (about 1/40 times the intensity of sunlight).[1] The length of the UV lamp is longer than our reactor, therefore only 2/3 of the lamp could be inserted into our reactor. As a result, to have an appropriate calculation, a light source of only 16 Watt was considered for this work. The hydrogen evolution experiments were carried out under steady stirring to continuously disperse the catalyst powder in solution. In our typical experiment, 225 mg catalyst powder was dispersed in 450 mL solution containing 10% ethanol to evolve hydrogen. During the photocatalytic hydrogen evolution experiments, the reactor was connected to a GC system with 99.99% Ar as the carrier gas. The flow rate of Ar gas was set to 100 mL $min^{-1}$ for the whole experiment. Prior to starting the lamp illumination, the reactor was purged with Ar gas for 1 h to remove all the

 

atmospheric gas remaining in the reactor. After the purging process, to ensure all atmospheric gas had been removed, a certain amount of gas from the reactor was initially checked by flowing it into the GC system. During the experiments, gas sampling was taken at the time interval of 30 min by flowing the evolved gas in the reactor into the GC system. The amount of produced hydrogen was determined based on the peak area in the GC spectra.

### 2.5 Photocatalytic reduction of 4-nitrophenol (4-NP) to 4-aminophenol (4-AP)

To reduce 4-NP to 4-AP, 225 mg catalyst powder was dispersed in 450 mL solution containing 10% ethanol and 30 ppm 4-NP. The Zn(O,S)/$Ga_2O_3$ nanocomposite catalyst, which showed the best hydrogen evolution performance, was used in this experiment. The photocatalytic reduction was carried out under a continuous flow of Ar gas through the reactor and under 4 × 6 Watt UV blacklight tube lamp illumination. Initially, to investigate whether the catalyst could perform the photocatalytic reduction, an aliquot was taken from the solution 15 min after turning on the UV lamps and was investigated using a UV-vis spectrophotometer. If the results from the UV-vis spectrophotometer showed a UV absorbance peak shift to 300 nm, indicating the formation of 4-AP, then the same procedure was conducted again and another aliquot was taken after 1 h for high-performance liquid chromatography (HPLC) measurements. The aliquots were taken for a period of 3 h and were checked using HPLC analysis to clearly reveal the reduction of 4-NP and the formation of 4-AP during the 3 h photoreaction.

## 3 Results and discussion

### 3.1 X-ray diffractometer (XRD) pattern of Zn(O,S)/$Ga_2O_3$ nanocomposite

To investigate the crystal structures of the Zn(O,S)/$Ga_2O_3$ nanocomposite, the as-prepared nanocomposite powders were examined using X-ray diffractometry. Fig. 1 shows the XRD patterns of the as-prepared $Ga_2O_3$, Zn(O,S)/0.5% $Ga_2O_3$, Zn(O,S)/3% $Ga_2O_3$, Zn(O,S)/5% $Ga_2O_3$, Zn(O,S)/10% $Ga_2O_3$ and Zn(O,S)/20% $Ga_2O_3$ powders compared to that of Zn(O,S). The as-prepared Zn(O,S) pattern shows a cubic structure with the main peaks located between those of ZnO (JCPDS #65-2880) and ZnS (JCPDS #05-0566), as shown in our previous work.[1] The peaks of the $Ga_2O_3$ phase gradually appeared with increasing amount of $Ga_2O_3$ in the nanocomposites. The major peaks of the $Ga_2O_3$ phase in the nanocomposites assigned to the (111), (−211) and (017) planes were in good agreement with the major peaks of as-prepared $Ga_2O_3$ as shown in Fig. 1. All the peaks of as-prepared $Ga_2O_3$ matched those in JCPDS #11-0370. However, a slight peak shift ($2\theta$ = 0.5°) to a higher angle was observed. This may due to lattice distortion during the low temperature preparation. The XRD patterns indicated that the Zn(O,S) and $Ga_2O_3$ phases were successfully synthesized at low temperature to form a nanocomposite powder. The broad peaks indicated in Fig. 1 confirmed that the nanocomposites contained tiny particles.

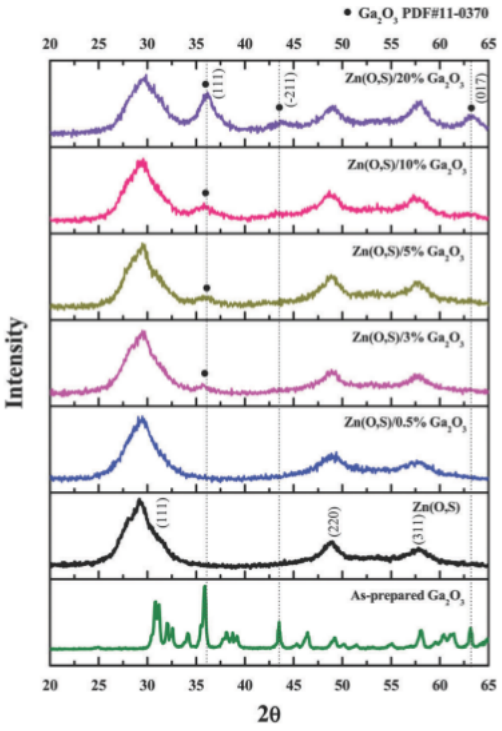


Fig. 1 XRD patterns of as-prepared $Ga_2O_3$ and Zn(O,S)/$Ga_2O_3$ nanocomposites with different $Ga_2O_3$ content.

The crystalline sizes of Zn(O,S) and $Ga_2O_3$ are 2.5 and 5.2 nm based on the Scherrer equation for the Zn(O,S)(111) and $Ga_2O_3$(311) peaks, respectively. The XRD characterization reveals that Zn(O,S)/$Ga_2O_3$ forms a robust nanocomposite due to its tiny particle size. As confirmed by energy dispersive spectra (EDS) analysis, the amount of $Ga_2O_3$ is relatively low in the nanocomposites. The $Ga_2O_3$ amount was not observable for the as-designed Zn(O,S)/0.5% $Ga_2O_3$ nanocomposite. However, the actual amounts of $Ga_2O_3$ in Zn(O,S)/3% $Ga_2O_3$, Zn(O,S)/5% $Ga_2O_3$, Zn(O,S)/10% $Ga_2O_3$ and Zn(O,S)/20% $Ga_2O_3$ were 0.06%, 0.55%, 1.58% and 4.08%, respectively, based on the EDS analysis.

### 3.2 Morphology and microstructure of Zn(O,S)/$Ga_2O_3$ nanocomposite

The morphology of the Zn(O,S)/$Ga_2O_3$ nanocomposites was examined using FE-SEM and the results are shown in Fig. S1 (ESI†). The sizes and shapes of the nanocomposites are similar to those of the Zn(O,S) nanoparticles. To clearly examine the nanocomposites, high-resolution transmission electron microscope (HRTEM) analysis was used to reveal the element mapping and lattice fringes of the Zn(O,S)/$Ga_2O_3$ phases. Fig. 2 shows the HRTEM analysis of element mapping, lattice fringes and selected area electron diffraction pattern (SAED) of the Zn(O,S)/10% $Ga_2O_3$ nanocomposite. The tiny particle size of the Zn(O,S)/10% $Ga_2O_3$ nanocomposite shown in Fig. 2a is consistent with the XRD analysis. All the elements of Zn, Ga, O and S in the Zn(O,S)/10% $Ga_2O_3$ nanocomposite are presented in Fig. 2b–e, respectively.

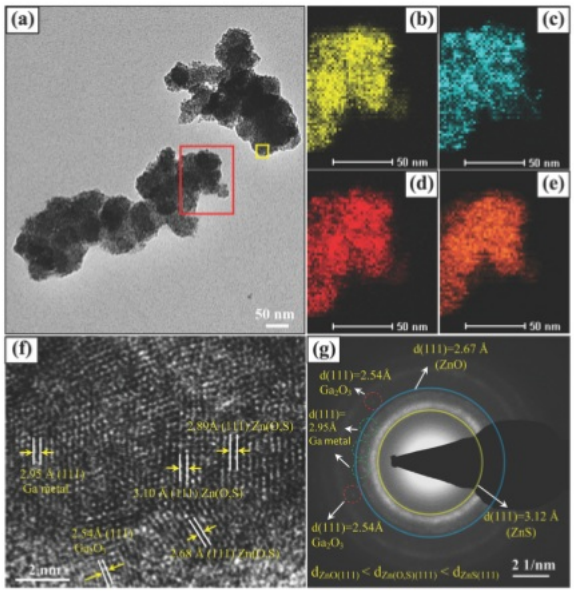


Fig. 2 High-resolution images of (a) Zn(O,S)/20% $Ga_2O_3$ nanocomposites with (b) Zn, (c) Ga, (d) O and (e) S element mapping from the red rectangle area in (a). (f) The lattice fringes of Ga metal, $Ga_2O_3$ and Zn(O,S) nanoparticles from the area indicated in the yellow rectangle in (a). (g) Selected area electron diffraction patterns (SAED) of the Zn(O,S) phase with a broad ring pattern at (111) located between the depicted ring patterns of ZnS and ZnO. The weak dot patterns of the $Ga_2O_3$ and Ga metal phases were also observable as indicated with the red and green circles, respectively.

The lattice fringe values of Zn(O,S) (JCPDS #65-2880; JCPDS #05-0566), $Ga_2O_3$ (JCPDS #11-0370) and Ga metal (JCPDF #05-0601) at (111) are 2.68–3.10 Å, 2.54 Å and 2.95 Å, respectively, as indicated in Fig. 2f. The lattice fringe values of Zn(O,S) at (111), which are between those of ZnO and ZnS, are consistent with our previous work.[1] The broad ring patterns of Zn(O,S)/10% $Ga_2O_3$ are also in agreement with our previous work.[1] However, the $Ga_2O_3$ pattern is not clearly shown in the SAED pattern due to its lower amount on the Zn(O,S) surface. The overlapping dot pattern of Ga metal and broad ring pattern of Zn(O,S) were confirmed with the lattice fringe of Ga metal, which was located in the range of the Zn(O,S) lattice fringes ($d_{ZnO(111)} < d_{Zn(O,S)(111)} < d_{ZnS(111)}$). The weak dot patterns of $Ga_2O_3$ and Ga metal indicated by the red and green circles were observable in the SAED pattern, as shown in Fig. 2g. A complete discussion about the formation of a Zn(O,S) solid solution in relation to the formation of a three dimensional multi-bandgap quantum well (3D MQW) has been well discussed in our previous work.[1] The HRTEM analysis reveals the formation of a composite containing nanosized Zn(O,S) and $Ga_2O_3$ phases with good interfaces between them. The good interface between the two phases, as indicated in Fig. 2f, is advantageous for electron transfer, to enhance the catalytic performance.

### 3.3 Diffuse reflectance spectra (DRS) analysis

Diffuse reflectance spectra (DRS) measurements were carried out to gain a better understanding of the Zn(O,S)/$Ga_2O_3$ nanocomposite properties. Fig. 3 shows the diffuse reflectance spectra of all the as-prepared nanocomposites. The results reveal that the highest absorbance is found in the UV range. Zn(O,S)/0.5% $Ga_2O_3$ has the highest UV light absorbance in the range between 240 and 340 nm, followed by Zn(O,S)/5% $Ga_2O_3$, Zn(O,S)/3% $Ga_2O_3$, Zn(O,S)/10% $Ga_2O_3$, Zn(O,S)/20% $Ga_2O_3$, Zn(O,S) and the as-prepared $Ga_2O_3$. However, it was observed that the nanocomposites containing the 0.5–10% $Ga_2O_3$ do not have significantly different UV light absorbances. The wavelength of the UV light source used in this work is about 352 nm, as indicated in Fig. 3. A higher energy UV lamp ($\lambda < 350$ nm) was not used in this work due to safety concerns. Based on the DRS measurements, the bandgap values of the Zn(O,S), Zn(O,S)/0.5% $Ga_2O_3$, Zn(O,S)/3% $Ga_2O_3$, Zn(O,S)/5% $Ga_2O_3$, Zn(O,S)/10% $Ga_2O_3$ and Zn(O,S)/20% $Ga_2O_3$ composites and the as-prepared $Ga_2O_3$ were 3.51, 3.59, 3.60, 3.57, 3.56, 3.53 and 4.78 eV, respectively, as shown in the ESI† (Fig. S3). It was noticed that the nanocomposite formation did not significantly influence the bandgap values; however, the UV light absorbance was obviously increased. As we observed, the light absorbance intensity of Zn(O,S) after being coupled with $Ga_2O_3$ was increased by 50% for Zn(O,S)/0.5% $Ga_2O_3$. The DRS measurements show that coupling Zn(O,S) and $Ga_2O_3$ led to a good synergy, which enhanced the optical properties in the range of 240–340 nm and probably would lead to enhancements to the photocatalytic reaction.

### 3.4 X-ray photoelectron spectroscopy (XPS) analysis

To confirm the chemical states of each element in the Zn(O,S)/$Ga_2O_3$ nanocomposites, the as-prepared Zn(O,S)/10% $Ga_2O_3$ nanocomposite was carefully examined using XPS analysis. XPS is a sensitive technique used to characterize the elemental composition at the parts per thousand range, chemical state and electronic state of the elements that exist on material surfaces. All the elements in the Zn(O,S)/$Ga_2O_3$ nanocomposite were found in the full scan XPS spectra as seen in Fig. S2 in the ESI.† Fig. 4 shows the high-resolution spectra of Zn, Ga, O and S elements in the nanocomposite. The binding energy values of Zn $2p_{1/2}$ and Zn $2p_{3/2}$ are noticed at 1045.7 eV and 1022.7 eV, respectively, which is in good agreement with the literature.[1,22]

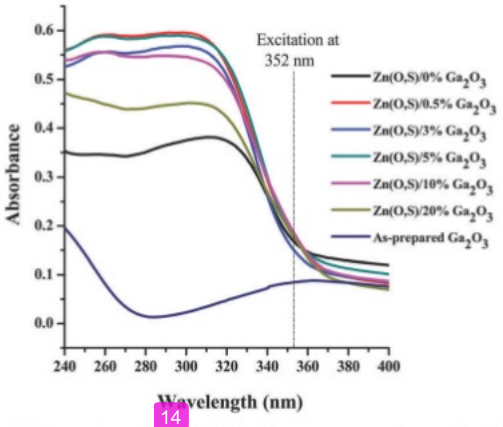


Fig. 3 DRS spectra of Zn(O,S)/$Ga_2O_3$ nanocomposites with different amounts of $Ga_2O_3$ and as-prepared $Ga_2O_3$ for comparison.

 

XPS measurements revealed that Ga in the nanocomposite was found not only in the oxide phase, but also in the metal phase. However, Ga metal peaks did not show up in the XRD patterns, as confirmed in Fig. 1, due to the relatively low amount of Ga metal in the nanocomposite. The binding energy values of Ga $2p_{1/2}$ and Ga $2p_{3/2}$ in the oxide phase were observed at 1145.6 and 1118.8 eV, respectively, while those of Ga (metal) $2p_{1/2}$ and Ga (metal) $2p_{3/2}$ were noticed at 1139.3 and 1113.6 eV, respectively.[22,23] The Ga metal phase was calculated to be 35% based on the total Ga content. Oxygen binding energy values of O 1s located at 530.1 and 531.1 eV were related to oxygen in the lattice and oxygen vacancies on the nanocomposite surfaces, respectively.[22,24] The amounts of lattice oxygen and oxygen vacancies were calculated to be 75% and 25%, respectively, based on the peak areas. The peaks of S $2p_{1/2}$ and S $2p_{3/5}$ were observed at 165.3 and 164.3 eV, which are in good agreement with previous works.[1,22] The XPS analysis confirmed the chemical state of each element in the Zn(O,S)/$Ga_2O_3$ nanocomposite including Ga metal, which was not observable in the XRD analysis. Additional XPS data for as-prepared $Ga_2O_3$ is also provided in the ESI† (Fig. S10) to confirm the chemical state of each element in $Ga_2O_3$. All the peaks for Ga 2p and O 1s are in good agreement with those of $Ga_2O_3$ in the nanocomposite.

### 3.5 Photocatalytic hydrogen evolution reaction (HER)

The photocatalytic HER was carried out in 10% ethanol solution for 5 h in the presence of 225 mg Zn(O,S)/$Ga_2O_3$ nanocomposite powder without a noble metal (Pt or Au) as a cocatalyst under 4 × 6 W UV light illumination. A gas sample was taken from the reactor in the time interval of 30 min by flowing 99.99% Ar gas through the reactor to a gas chromatography (GC) system. Fig. 5 shows the amount of hydrogen evolved during the HER experiment using Zn(O,S)/$Ga_2O_3$ nanocomposites with different $Ga_2O_3$ content, as-prepared $Ga_2O_3$ and commercially available P25 as a standard catalyst for comparison. In many other previous works,[25–27] $TiO_2$ has been shown to be a great catalyst for evolving hydrogen. However, noble metals such as Pt have been needed to trap electrons and efficiently enhance the lifetime of photo-carriers, otherwise no hydrogen gas is evolved, as shown in Fig. 5. Furthermore, in those reported works, toxic hole-scavenger reagents, such as $Na_2S$, have been commonly used. Furthermore, only a small amount of hydrogen can be evolved in aqueous solution in the presence of Pt/$TiO_2$. Our experimental results show that Zn(O,S)/$Ga_2O_3$ with low $Ga_2O_3$ content was not effective for hydrogen evolution, and this might be caused by the limited degree of heterojunction formation, leading to ineffective electron transfer during the photoreaction. The photocatalytic activity of Zn(O,S) is higher than that of the nanocomposites with 0.5–5% $Ga_2O_3$. A related observation in the DRS spectra at 352 nm also showed lower absorbance for lower $Ga_2O_3$ content (0.5–5%). $Ga_2O_3$ is a wide bandgap material; therefore the light absorbance and photocatalytic activity was lower as higher wavelength

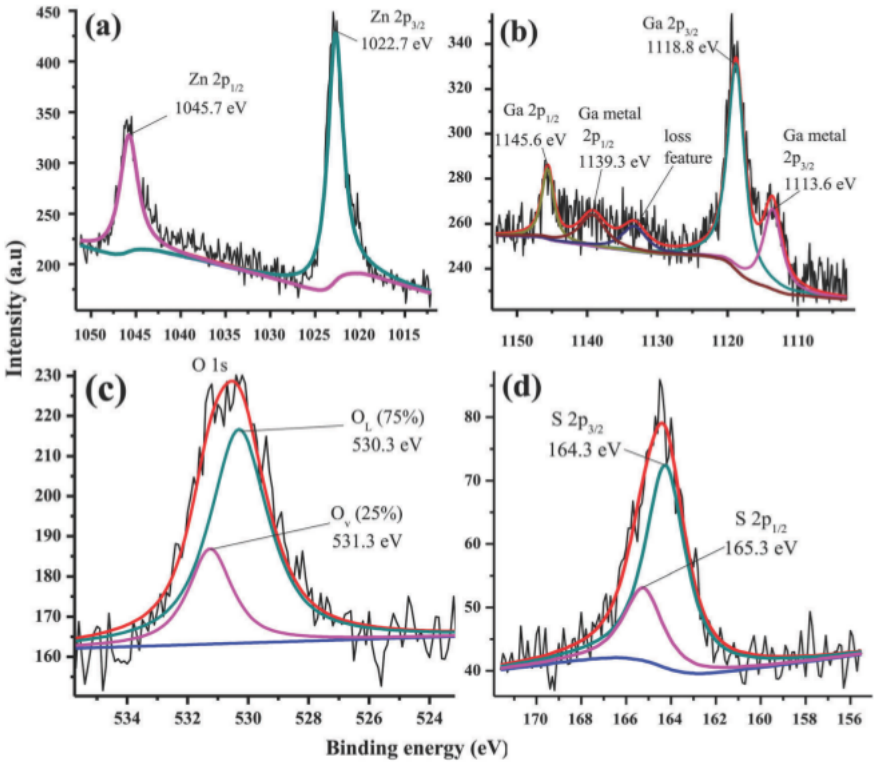


Fig. 4 High-resolution XPS spectra of (a) Zn 2p, (b) Ga 2p, (c) O 1s and (d) S 2p peaks for the Zn(O,S)/10% $Ga_2O_3$ nanocomposites.

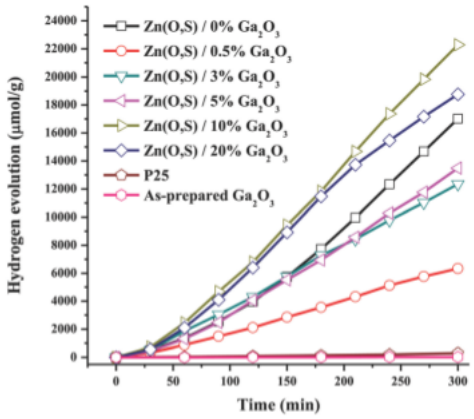


Fig. 5 Photocatalytic hydrogen evolution in 10% ethanol solution catalyzed by Zn(O,S)/$Ga_2O_3$ nanocomposites with different contents of $Ga_2O_3$ and as-prepared $Ga_2O_3$ under 24 W UV tube lamp illumination.

photons (352 nm) were used to illuminate the photocatalysts. When a lower amount of $Ga_2O_3$ was used, there was no synergetic effect between the Zn(O,S) and $Ga_2O_3$ phases. This might be related to the lower background absorbance of $Ga_2O_3$ and inefficient electron transfer in the interface between the two phases using 352 nm wavelength illumination. With an increasing amount of $Ga_2O_3$ in the nano-heterostructure composites, the background absorbance gradually increased and became higher than that of Zn(O,S), particularly at the wavelength of 352 nm, as shown in the DRS spectra. The experimental data revealed that an optimum synergistic effect was achieved at 10% $Ga_2O_3$ content in Zn(O,S)/$Ga_2O_3$. To show the inefficient electron transfer in the nanocomposites of lower $Ga_2O_3$ content, electrochemical impedance spectroscopy (EIS) measurements were carried out for all the catalysts. The results reveal a higher resistance and inefficient electron transfer for the nanocomposites with lower $Ga_2O_3$ content. Higher resistance corresponded to a larger arc profile in the EIS spectra, as shown in the ESI† (Fig. S8). The Randles equivalent circuit was used to fit the experimental data. Based on the Randles fitting, the calculated electron transfer resistance values of Zn(O,S), Zn(O,S)/0.5% $Ga_2O_3$, Zn(O,S)/3% $Ga_2O_3$, Zn(O,S)/5% $Ga_2O_3$, Zn(O,S)/10% $Ga_2O_3$, Zn(O,S)/20% $Ga_2O_3$ and $Ga_2O_3$ were 55.7 kΩ, 91.3 kΩ, 77.85 kΩ, 71.8 kΩ, 36.5 kΩ, 43.8 kΩ and 98.0 kΩ, respectively. The lowest resistance observed for Zn(O,S)/10% $Ga_2O_3$ indicated the most efficient electron transfer on the interfaces between the catalyst and electrolyte during the photocatalytic reaction for hydrogen production. The highest hydrogen amount of 280 μmol $g^{-1}$ $h^{-1}$ $W^{-1}$ was achieved in the presence of the Zn(O,S)/10% $Ga_2O_3$ nanocomposite, as shown in Fig. 5. With Zn(O,S) coupled to $Ga_2O_3$, the amount of hydrogen evolved was increased by 30%, as compared to our previous work.[1] Increasing the $Ga_2O_3$ content to 20% lowered the photocatalytic performance, possibly due to the coverage of higher bandgap $Ga_2O_3$ on Zn(O,S) surfaces, lowering the amount of photo-generated electrons and decreasing the efficiency of HER.[28] The experimental data show that a relatively small amount of $Ga_2O_3$ (only 1.58% as indicated by the EDS analysis) in the nanocomposites could significantly enhance the photocatalytic HER, even without utilizing a noble metal or toxic hole-scavenger reagent. To gain a deeper understanding of our photocatalysts, the surface areas of the Zn(O,S), Zn(O,S)/0.5% $Ga_2O_3$, Zn(O,S)/3% $Ga_2O_3$, Zn(O,S)/5% $Ga_2O_3$, Zn(O,S)/10% $Ga_2O_3$ and Zn(O,S)/20% $Ga_2O_3$ composites and as-prepared $Ga_2O_3$ were examined, and the results are shown in Table 1.

The BET results show that the surface areas of the nanocomposites increase as the $Ga_2O_3$ content increases. However, a 20% $Ga_2O_3$ content in the nanocomposite induces a lower surface area, which might be related to $Ga_2O_3$ nanoparticle aggregation. It was found that the highest surface area of Zn(O,S)/$Ga_2O_3$ is obviously increased by more than 7 times due to the incorporation of $Ga_2O_3$ to form the nanocomposite photocatalyst. Therefore, the nanocomposite formation and the enhanced surface area simultaneously increase the reactive photocatalytic sites.

### 3.6 Utilization of hydrogen evolution Zn(O,S)/$Ga_2O_3$ nanocomposites for 4-NP reduction

To evaluate the potential of the hydrogen evolution photocatalysts for environmental remediation, the as-prepared Zn(O,S)/10% $Ga_2O_3$ nanocomposite was utilized to reduce 30 ppm 4-NP in 10% ethanol solution under low-intensity UV light illumination. The reduction reaction was carried out in an Ar atmosphere with a continuous flow of Ar gas during the experiment to eliminate any effects from atmospheric gas. In this experiment, 225 mg Zn(O,S)/10% $Ga_2O_3$ nanocomposite powder was well dispersed in 450 mL 4-NP solution. To understand the photocatalytic reduction of 4-NP on the Zn(O,S)/10% $Ga_2O_3$ nanocomposite, the experiments were carried out under different conditions. Fig. 6 shows four kinds of experiments with 30 ppm 4-NP conducted in 10% ethanol solution with the Zn(O,S) or $Ga_2O_3$ catalyst, in Zn(O,S)/10% $Ga_2O_3$ catalyst-dispersed pure water, and in 10% ethanol solution with dispersed Zn(O,S)/10% $Ga_2O_3$ catalyst. There were no changes in the UV-vis absorbance for the aliquots taken from the solution containing only 4-NP and 10% ethanol after illumination with a UV lamp for 90 min, as shown in Fig. S5 in the ESI.† The experiment with single phases of Zn(O,S) and $Ga_2O_3$ did not significantly exhibit the reduction of 4-NP in ethanol solution as shown in Fig. 6a and b. The experiment with 30 ppm 4-NP in Zn(O,S)/10% $Ga_2O_3$-dispersed pure water showed absorbance peak shifts

Table 1 Surface areas of Zn(O,S)/$Ga_2O_3$ nanocomposites with different amounts of $Ga_2O_3$ and as-prepared $Ga_2O_3$

| | Photocatalysts | | | | | | |
|---|---|---|---|---|---|---|---|
| BET results | Zn(O,S) | Zn(O,S)/0.5% $Ga_2O_3$ | Zn(O,S)/3% $Ga_2O_3$ | Zn(O,S)/5% $Ga_2O_3$ | Zn(O,S)/10% $Ga_2O_3$ | Zn(O,S)/20% $Ga_2O_3$ | $Ga_2O_3$ |
| Surface area ($m^2$ $g^{-1}$) | 18.77 | 33.76 | 68.50 | 87.62 | 137.22 | 102.35 | 130.07 |

 

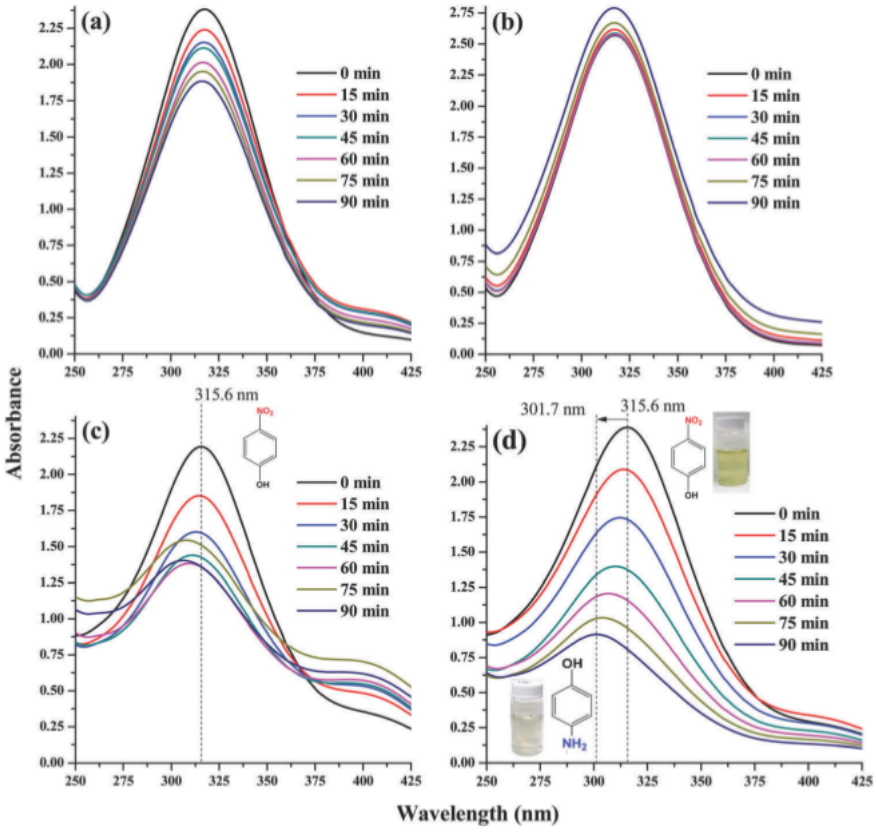


Fig. 6 UV-vis absorbance spectra of (a) 30 ppm 4-NP + 10% ethanol solution + Zn(O,S), (b) 30 ppm 4-NP + 10% ethanol solution + $Ga_2O_3$, (c) 30 ppm 4-NP + Zn(O,S)/$Ga_2O_3$ catalyst, and (d) 30 ppm 4-NP + 10% ethanol solution + Zn(O,S)/$Ga_2O_3$ catalyst with different 24 W UV-light illumination periods.

after illumination with a UV lamp for more than 30 min, as shown in Fig. 6c. However, the peak shifts occurred slowly and improperly. This result might be due to a lower hydrogen evolution rate in pure water without ethanol as a hole-scavenger agent.[1] The last experiment with 30 ppm 4-NP in Zn(O,S)/10% $Ga_2O_3$-dispersed ethanol (10%) solution showed a smooth peak shift from 315.6 to 301.7 nm in 90 min. The absorbance peaks at 315.6 nm and 301.7 nm were respectively related to 4-NP and 4-AP absorbances in solution.[10] The related solution images at those peaks of 315.6 nm and 301.7 nm are also shown in the inset in Fig. 6d. After 90 min of the reduction reaction, the solution changed from yellowish (4-NP) to clear (4-AP). The experiments confirmed that the photocatalytic reduction of 4-NP to 4-AP occurred in the presence of the Zn(O,S)/10% $Ga_2O_3$ catalyst in 10% ethanol solution. This result indicates the important role of ethanol as a hole-scavenger reagent in enhancing the photocatalytic reduction of 4-NP.

### 3.7 High-performance liquid chromatography (HPLC) analysis

Aliquots from the reduction experiment involving 30 ppm 4-NP in Zn(O,S)/10% $Ga_2O_3$-dispersed ethanol (10%) solution were investigated using HPLC analysis. To separate 4-NP and 4-AP in the aliquots, a reversed-phase liquid chromatography C-18 column with a mobile phase of a 20% methanol solution containing 5 mM tetrabutylammonium phosphate (TBAP) was used in the HPLC measurement. The 4-NP in solution was detected with a UV detector at 323 nm, while 4-AP in solution was detected with a fluorescent detector for the 423 nm emission after excitation at 300 nm. The measurement was run at room temperature with a flow rate of 1 mL $min^{-1}$ and the sample intake was 50 μL for all aliquots. To determine the 4-NP and 4-AP retention times, commercially available 4-NP and 4-AP standard solutions were used in the measurement. It was found that the retention times were 28 min for 4-NP and 5 min for 4-AP with UV and fluorescent detectors, respectively. Fig. 7 shows the chromatograms with a decreased peak intensity for 4-NP and an increased peak intensity for 4-AP after the reactions had proceeded from 0 to 3 h, as shown in Fig. 7a and b, respectively. Based on the peak height in Fig. 7a, the remaining concentrations of 4-NP in solution were 100%, 33.8%, 23.1% and 13.0% after reactions for 0, 1, 2 and 3 h, respectively. The HPLC results confirm the formation of 4-AP as a product of 4-NP reduction. To show the synergetic effect between Zn(O,S) and $Ga_2O_3$ in the nanocomposite with enhanced photocatalytic activity, 4-NP reduction experiments with HPLC analysis were separately conducted for Zn(O,S) and $Ga_2O_3$. The results indicate lower photocatalytic 4-NP

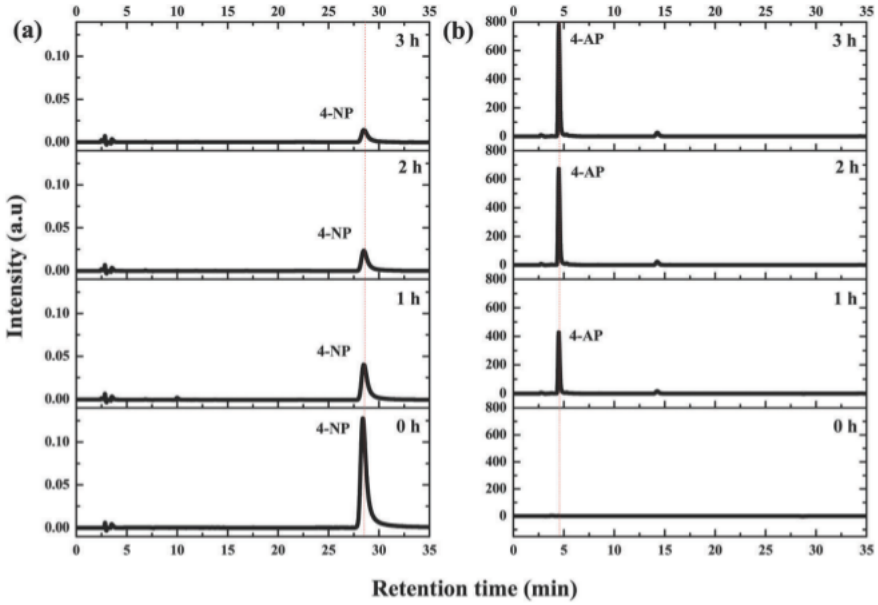


Fig. 7 High-performance liquid chromatograms (HPLC) of (a) 4-NP and (b) 4-AP solutions after photocatalytic reduction reaction in the presence of the Zn(O,S)/10% $Ga_2O_3$ nanocomposite with different photoreaction times using UV and fluorescence detectors, respectively.

conversion rates to form 4-AP for Zn(O,S) and $Ga_2O_3$ as shown in Fig. S6 and S7 (ESI†), respectively.

### 3.8 Photocatalytic mechanisms of hydrogen evolution reaction and 4-NP reduction

The main mechanisms by which the Zn(O,S) nanoparticles evolve hydrogen under UV light illumination have been elucidated in our previous work.[1] In this work, the enhanced photocatalytic performance is related to efficient electron transfer between Zn(O,S) and $Ga_2O_3$ phases due to different flat band potentials leading to better photo-carrier separation.[12,29] The Ga metal, as confirmed by XPS analysis, might play a role in enhancing the photocatalytic activity by trapping electrons during photoreaction, due to its comparable work function with Ag.[30–32] To draw the band structure of the Zn(O,S)/$Ga_2O_3$ nanocomposite, Mott–Schottky measurements were carried out (Fig. S4 in the ESI†) to determine the flat band potential of each phase in the nanocomposites using glassy carbon, platinum and Ag/AgCl electrodes as working, counter and reference electrodes, respectively.[3,34] Based on previous works[1,28] and the DRS measurements in this work, the bandgap values of Zn(O,S) and as-prepared $Ga_2O_3$ were determined to be about 3.60 and 4.78 eV, respectively. Fig. 8 presents the heterojunction band diagram of the Zn(O,S)/$Ga_2O_3$ nanocomposite with a typical straddling gap, which induces the electrons and holes from $Ga_2O_3$ to transfer to the conduction and valence bands of Zn(O,S), respectively. It is believed that some defect states in the $Ga_2O_3$ conduction band are involved in producing the photo-generated electrons due to oxygen vacancy formation during the low temperature process.[1] A small intensity increase in the absorbance of as-prepared $Ga_2O_3$ in the DRS spectra was also observable at 352 nm, as shown in Fig. 3, which implies the possibility for electrons to be excited at this region. Furthermore, to show the possibility that a defect state occurred during $Ga_2O_3$ formation, a photoluminescence (PL) experiment was carried out for as-prepared $Ga_2O_3$ and the results are shown in the ESI† (Fig. S9). It was found that a small broad peak showed up in the range of 350–400 nm that was located at the excitation range of our UV tube lamp illumination, meaning that it was possible to excite the as-prepared $Ga_2O_3$ with 352 nm photons. The peak at 350–4[illegible]nm in the PL spectra was related to the emission intensity due to the recombination process between photo-excited electrons and holes at a specific state level. The low emission intensity indicates that only a few electrons were excited during the photocatalytic session. However, after photo-excitation, the photo-carriers of the $Ga_2O_3$ conduction and valence bands would drift towards those of Zn(O,S) due to the in-built electric field between them. This in-built electric field is important to separate the electrons and holes after photo-excitation and to enhance the photo-carrier lifetime.[17,18] If the lifetime of the photo-carriers was longer than that of the photoreaction, then photocatalytic hydrogen evolution or reduction would be improved. As there would be more photo-generated electrons and holes in the Zn(O,S) conduction and valence bands, respectively, further photocatalytic hydrogen evolution reaction would mainly occur on Zn(O,S) surfaces, as elucidated in our previous work.[1] It was observed that the photocatalytic hydrogen evolution reaction was initiated by water oxidation with surface oxygen anions to form oxygen vacancy sites on the catalyst surfaces, as shown in Fig. 8. Furthermore, the oxygen vacancy sites were enhanced if ethanol was available in the solution. The active oxygen vacancy sites were very crucial for water reduction to form $H_2$ and surface oxygen anions.[1] However,

 

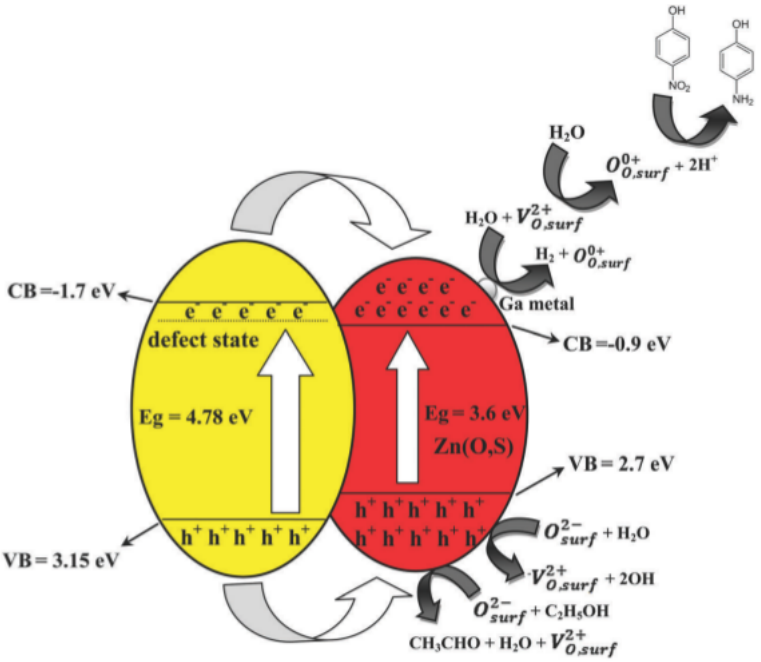


Fig. 8 A typical straddling gap of Zn(O,S)/$Ga_2O_3$ heterojunction with Fermi level alignment.

the oxygen vacancy sites were also consumed by the reaction to form hydrogen ions that are critical to reduce 4-NP to 4-AP. Therefore, the hydrogen evolution rate significantly decreases as long as 4-NP is available in the solution, as shown in Fig. 9. This reveals that the produced hydrogen amount in the presence of 4-NP was significantly lower compared to that in ethanol solution because the produced hydrogen ions were consumed by the 4-NP reduction reaction. It is well known that the availability of hydrogen ions that evolve on catalyst surfaces is a crucial step to reduce 4-NP.[5,8–10]

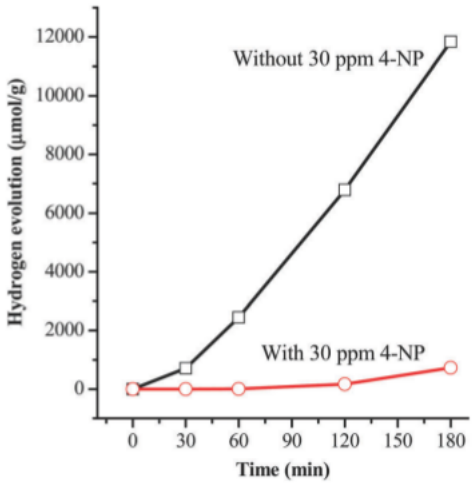


Fig. 9 Photocatalytic hydrogen evolution in the presence of Zn(O,S)/10% $Ga_2O_3$ nanocomposites in 10% ethanol solution with and without 30 ppm 4-NP.

## 4 Conclusions

A one-pot synthesis of Zn(O,S)/$Ga_2O_3$ nanocomposites with different amounts of $Ga_2O_3$ was carried out and the as-prepared nanocomposite powders were characterized using XRD, FE-SEM, HRTEM, DRS, BET, EIS and XPS analysis. The Zn(O,S)/10% $Ga_2O_3$ nanocomposite exhibited the best performance with a hydrogen production rate of 280 μmol $g^{-1}$ $h^{-1}$ $W^{-1}$. The enhanced photocatalytic performance of the Zn(O,S)/$Ga_2O_3$ nanocomposite is related to efficient electron transfer between the Zn(O,S) and $Ga_2O_3$ phases, which form a straddling gap to increase the amount of photo-carriers in the photoreaction. It was confirmed that the formation of the Zn(O,S)/$Ga_2O_3$ heterojunction significantly increased the hydrogen evolution rate by 30%, as compared with the single Zn(O,S) phase. During the photoreaction, the hydrogen ions generated on the nanocomposite surfaces could be utilized for 4-NP reduction to form 4-AP. The reduction of 4-NP on the Zn(O,S)/$Ga_2O_3$ nanocomposite was confirmed using UV-vis spectroscopy, HPLC measurements, and the decreased amount of evolved hydrogen that was consumed in the 4-NP reduction. Finally, it is concluded that the Zn(O,S)/$Ga_2O_3$ nanocomposites can simultaneously generate hydrogen and remediate the toxic pollutant 4-NP in ethanol solution under low UV light illumination (0.088 mW $cm^{-2}$ or approximately 1/40-fold UV light intensity of sunlight).

## 5 Conflicts of interest

There are no conflicts to declare.

## Acknowledgements

This work was supported by the Ministry of Science and Technology of Taiwan under Grant numbers MOST 105-2218-E-011-013 and MOST 106-3111-Y-042A-093.

## References

1 H. Abdullah, D.-H. Kuo and X. Chen, *Int. J. Hydrogen Energy*, 2017, **42**, 5638–5648.
2 Y. Tamaki and O. Ishitani, *ACS Catal.*, 2017, 3394–3409, DOI: 10.1021/acscatal.7b00440.
3 P. Kalisman, Y. Nakibli and L. Amirav, *Nano Lett.*, 2016, **16**, 1776–1781.
4 R. Shiratsuchi, K. Hongo, G. Nogami and S. Ishimaru, *J. Electrochem. Soc.*, 1992, **139**, 2544–2549.
5 D. Xu, P. Diao, T. Jin, Q. Wu, X. Liu, X. Guo, H. Gong, F. Li, M. Xiang and Y. Ronghai, *ACS Appl. Mater. Interfaces*, 2015, **7**, 16738–16749.
6 J. F. Corbett, *Dyes Pigm.*, 1999, **41**, 127–136.
7 L. Lunar, D. Sicilia, S. Rubio, D. Pérez-Bendito and U. Nickel, *Water Res.*, 2000, **34**, 1791–1802.
8 Y.-C. Chang and D.-H. Chen, *J. Hazard. Mater.*, 2009, **165**, 664–669.
9 M. M. Mohamed and M. S. Al-Sharif, *Appl. Catal., B*, 2013, **142–143**, 432–441.
10 O. Ahmed Zelekew and D.-H. Kuo, *Phys. Chem. Chem. Phys.*, 2016, **18**, 4405–4414.
11 Q. Deng, H. Tang, G. Liu, X. Song, G. Xu, Q. Li, D. H. L. Ng and G. Wang, *Appl. Surf. Sci.*, 2015, **331**, 50–57.
12 R. M. Navarro Yerga, M. C. Álvarez Galván, F. del Valle, J. A. Villoria de la Mano and J. L. G. Fierro, *ChemSusChem*, 2009, **2**, 471–485.
13 G. Heidari, M. Rabani and B. Ramezanzadeh, *Int. J. Hydrogen Energy*, 2017, **42**, 9545–9552.
14 M. Sohail, H. Xue, Q. Jiao, H. Li, K. Khan, S. Wang and Y. Zhao, *Mater. Res. Bull.*, 2017, **90**, 125–130.
15 T.-F. Hou, R. Boppella, A. Shanmugasundaram, D. H. Kim and D.-W. Lee, *Int. J. Hydrogen Energy*, 2017, **42**, 15126–15139.
16 X. Zhou, H. Dong and A.-M. Ren, *Int. J. Hydrogen Energy*, 2016, **41**, 5670–5681.
17 H. Abdullah and D.-H. Kuo, *ACS Appl. Mater. Interfaces*, 2015, **7**, 26941–26951.
18 H. Abdullah and D.-H. Kuo, *J. Phys. Chem. C*, 2015, **119**, 13632–13641.
19 H. Abdullah, D.-H. Kuo, Y.-R. Kuo, F.-A. Yu and K.-B. Cheng, *J. Phys. Chem. C*, 2016, **120**, 7144–7154.
20 Y. Wang, P. H. C. Camargo, S. E. Skrabalak, H. Gu and Y. Xia, *Langmuir*, 2008, **24**, 12042–12046.
21 D. Zhang, P. Diao and Q. Zhang, *J. Phys. Chem. C*, 2009, **113**, 15796–15800.
22 J. F. Moulder, J. Chastain and R. C. King, *Physical Electronics*, Eden Prairie, MN, 1995.
23 J. Wipakorn, M. Tatsuro, M. Noriyuki, O. Minoru, I. Toshifumi, T. Tsutomu and Y. Tetsuji, *Appl. Phys. Express*, 2014, **7**, 011201.
24 B.-W. Huang, C.-Y. Wen, G.-W. Lin, P.-Y. Chen, Y.-H. Jiang, P.-K. Kao, C.-T. Chi, H. Chang, I. C. Cheng and J.-Z. Chen, *J. Am. Ceram. Soc.*, 2015, **98**, 125–129.
25 I. Rossetti, *ISRN Chem. Eng.*, 2012, **2012**, 1–21.
26 J. Jitputti, Y. Suzuki and S. Yoshikawa, *Catal. Commun.*, 2008, **9**, 1265–1271.
27 A. L. Luna, D. Dragoe, K. Wang, P. Beaunier, E. K. Kowalska, B. Ohtani, D. Bahena Uribe, M. A. Valenzuela, H. Remita and C. Colbeau-Justin, *J. Phys. Chem. C*, 2017, **121**, 14302–14311.
28 V. I. N. S. I. Stepanov, V. E. Bougrov and A. E. Romanov, *Rev. Adv. Mater. Sci.*, 2016, **44**, 63–86.
29 Y.-X. Pan, H. Zhuang, J. Hong, Z. Fang, H. Liu, B. Liu, Y. Huang and R. Xu, *ChemSusChem*, 2014, **7**, 2537–2544.
30 E. L. Ratcliff, A. K. Sigdel, M. R. Macech, K. Nebesny, P. A. Lee, D. S. Ginley, N. R. Armstrong and J. J. Berry, *Thin Solid Films*, 2012, **520**, 5652–5663.
31 J. C. Rivière, *Mino Green*, Marcel Dekker, New York, 1969, vol. 1.
32 *Springer Tracts in Modern Physics*, ed. J. Hölzl, F. K. Schulte and H. Wagner, Springer, Berlin, 1979, vol. 85.
33 N. Bhandary, A. P. Singh, P. P. Ingole and S. Basu, *RSC Adv.*, 2016, **6**, 35239–35247.
34 B. Mukherjee, A. Peterson and V. Subramanian, *Chem. Commun.*, 2012, **48**, 2415–2417.

 

ORIGINALITY REPORT

| 24% | 13% | 20% | 14% |
|---|---|---|---|
| SIMILARITY INDEX | INTERNET SOURCES | PUBLICATIONS | STUDENT PAPERS |

PRIMARY SOURCES

| | | |
|---|---|---|
| 1 | Submitted to School of Business and Management ITB<br>Student Paper | 2% |
| 2 | C. Platzer-Björkman, T. Törndahl, D. Abou-Ras, J. Malmström, J. Kessler, L. Stolt. "Zn(O,S) buffer layers by atomic layer deposition in Cu(In,Ga)Se2 based thin film solar cells: Band alignment and sulfur gradient", Journal of Applied Physics, 2006<br>Publication | 2% |
| 3 | Submitted to University of Science and Technology<br>Student Paper | 2% |
| 4 | link.springer.com<br>Internet Source | 2% |
| 5 | Noto Susanto Gultom, Hairus Abdullah, Dong-Hau Kuo. "Facile synthesis of cobalt-doped (Zn,Ni)(O,S) as an efficient photocatalyst for hydrogen production", Journal of the Energy Institute, 2019<br>Publication | 1% |

| | | |
|---|---|---|
| 6 | www.mdpi.com<br>Internet Source | 1% |
| 7 | Osman Ahmed Zelekew, Dong-Hau Kuo. "Facile synthesis of SiO2@CuxO@TiO2 heterostructures for catalytic reductions of 4-nitrophenol and 2-nitroaniline organic pollutants", Applied Surface Science, 2017<br>Publication | 1% |
| 8 | Submitted to Indian Institute of Foreign Trade<br>Student Paper | <1% |
| 9 | Submitted to SASTRA University<br>Student Paper | <1% |
| 10 | Osman Ahmed Zelekew, Dong-Hau Kuo. "Synthesis of a hierarchical structured NiO/NiS composite catalyst for reduction of 4-nitrophenol and organic dyes", RSC Advances, 2017<br>Publication | <1% |
| 11 | jmrt.com.br<br>Internet Source | <1% |
| 12 | Lijing Wang, Hongju Zhai, Gan Jin, Xiaoying Li, Chunwei Dong, Hao Zhang, Haiming Xie, Bai Yang, haizhu sun. "3D porous ZnO-SnS p-n heterojunction for visible light driven photocatalysis", Phys. Chem. Chem. Phys., 2017<br>Publication | <1% |

| | | |
|---|---|---|
| 13 | Uhm, Gi-Ryung, Shin Young Jang, Yong Han Jeon, Hee Kyung Yoon, and Hyungtak Seo. "Optimized electronic structure of a Cu(In,Ga)Se2 solar cell with atomic layer deposited Zn(O,S) buffer layer for high power conversion efficiency", RSC Advances, 2014.<br>Publication | <1% |
| 14 | Seung Wook Shin, M.P. Suryawanshi, Hee Kyeung Hong, Gun Yun, DongHa Lim, Jaeyeong Heo, Soon Hyung Kang, Jin Hyeok Kim. "Strategy for enhancing the solar-driven water splitting performance of TiO 2 nanorod arrays with thin Zn(O,S) passivated layer by atomic layer deposition", Electrochimica Acta, 2016<br>Publication | <1% |
| 15 | Michelle Navarrete, Sandra Cipagauta-Díaz, Ricardo Gómez. " Ga O /TiO semiconductors free of noble metals for the photocatalytic hydrogen production in a water/methanol mixture ", Journal of Chemical Technology & Biotechnology, 2019<br>Publication | <1% |
| 16 | Submitted to VIT University<br>Student Paper | <1% |
| 17 | Submitted to University College London<br>Student Paper | <1% |

| | | |
|---|---|---|
| 18 | Hairus Abdullah, Noto Susanto Gultom, Dong-Hau Kuo. "Indium oxysulfide nanosheet photocatalyst for the hexavalent chromium detoxification and hydrogen evolution reaction", Journal of Materials Science, 2017<br>Publication | <1% |
| 19 | Zarick, Holly F., William R. Erwin, Jayde Aufrecht, Andrew Coppola, Bridget R. Rogers, Cary L. Pint, and Rizia Bardhan. "Morphological modulation of bimetallic nanostructures for accelerated catalysis", Journal of Materials Chemistry A, 2014.<br>Publication | <1% |
| 20 | www.rsc.org<br>Internet Source | <1% |
| 21 | hal.laas.fr<br>Internet Source | <1% |
| 22 | Submitted to Higher Education Commission Pakistan<br>Student Paper | <1% |
| 23 | Submitted to Sardar Vallabhbhai National Inst. of Tech.Surat<br>Student Paper | <1% |
| 24 | Jianying Yu, Shixiang Lu, Wenguo Xu, Ge He, Dongsheng He. "Synthesis of gold/polydopamine composite surfaces on glass | <1% |

substrates for localized surface plasmon resonance and catalysis", Applied Organometallic Chemistry, 2017
Publication

| | | |
|---|---|---|
| 25 | Y. Arata, H. Nishinaka, D. Tahara, M. Yoshimoto. " Heteroepitaxial growth of single-phase ε-Ga O thin films on -plane sapphire by mist chemical vapor deposition using a NiO buffer layer ", CrystEngComm, 2018<br>Publication | <1% |
| 26 | www.hoghimwei.com<br>Internet Source | <1% |
| 27 | Submitted to Imperial College of Science, Technology and Medicine<br>Student Paper | <1% |
| 28 | Ioannis Vamvasakis, Bin Liu, Gerasimos S. Armatas. "Size Effects of Platinum Nanoparticles in the Photocatalytic Hydrogen Production Over 3D Mesoporous Networks of CdS and Pt Nanojunctions", Advanced Functional Materials, 2016<br>Publication | <1% |
| 29 | Submitted to IIT Delhi<br>Student Paper | <1% |
| 30 | Shuai Yang, Shurong Wang, Hua Liao, Xin Xu, Zhen Tang, Xinyu Li, Xiang Li, Tingbao Wang, Di Liu. "Sulfurizing Sputtered-ZnO as buffer | <1% |

layer for cadmium-free Cu2ZnSnS4 solar cells", Materials Science in Semiconductor Processing, 2019
Publication

| | | |
|---|---|---|
| 31 | sinta3.ristekdikti.go.id<br>Internet Source | <1% |
| 32 | www.beilstein-journals.org<br>Internet Source | <1% |
| 33 | Guangyou Pan, Jianhui Chen, Kunpeng Ge, Linlin Yang et al. "Zn(O,S)-based electron-selective contacts with tunable band structure for silicon heterojunction solar cells", Journal of Materials Chemistry C, 2019<br>Publication | <1% |
| 34 | Submitted to National University of Singapore<br>Student Paper | <1% |
| 35 | Noto Susanto Gultom, Hairus Abdullah, Dong-Hau Kuo. "Phase transformation of bimetal zinc nickel oxide to oxysulfide photocatalyst with its exceptional performance to evolve hydrogen", Applied Catalysis B: Environmental, 2020<br>Publication | <1% |
| 36 | "A New Generation Material Graphene: Applications in Water Technology", Springer Science and Business Media LLC, 2019<br>Publication | <1% |

| | | |
|---|---|---|
| 37 | Ye Tian, Yan-yan Cao, Fu Pang, Gui-qiang Chen, Xiao Zhang. "Ag nanoparticles supported on N-doped graphene hybrids for catalytic reduction of 4-nitrophenol", RSC Adv., 2014<br>Publication | <1% |
| 38 | Misganaw Alemu Zeleke, Dong-Hau Kuo, Kedir Ebrahim Ahmed, Noto Susanto Gultom. "Facile Synthesis of Bimetallic (In,Ga) 2 (O,S) 3 Oxy-Sulfide Nanoflower and Its Enhanced Photocatalytic Activity for Reduction of Cr(VI)", Journal of Colloid and Interface Science, 2018<br>Publication | <1% |
| 39 | magneticmicrosphere.com<br>Internet Source | <1% |
| 40 | repository.wima.ac.id<br>Internet Source | <1% |
| 41 | Sabrina Guimarães Sanches, Jhonny Huertas Flores, Maria Isabel Pais da Silva. "Influence of Ti source on the Ti-HMS photocatalyst synthesis used in a water splitting reaction", Materials Research Bulletin, 2019<br>Publication | <1% |
| 42 | Submitted to Visvesvaraya Technological University, Belagavi<br>Student Paper | <1% |
| 43 | M. Singh, K. Manoli, A. Tiwari, T. Ligonzo, C. Di | |

Franco, N. Cioffi, G. Palazzo, G. Scamarcio, L. Torsi. "The double layer capacitance of ionic liquids for electrolyte gating of ZnO thin film transistors and effect of gate electrodes", Journal of Materials Chemistry C, 2017 <1%
Publication

44 Zhixiong Liu, Shu Tian, Qiang Li, Jiancheng Wang, Jibin Pu, Gang Wang, Wenjie Zhao, Feng Feng, Jun Qin, Lichun Ren. "Integrated Dual-Functional ORMOSIL Coatings with AgNPs@rGO Nanocomposite for Corrosion Resistance and Antifouling Applications", ACS Sustainable Chemistry & Engineering, 2020 <1%
Publication

45 Submitted to Panjab University <1%
Student Paper

46 Submitted to University of Ulster <1%
Student Paper

47 Hairus Abdullah, Dong-Hau Kuo, Yen-Rong Kuo, Fu-An Yu, Kou-Bin Cheng. " Facile Synthesis and Recyclability of Thin Nylon Film-Supported -Type ZnO/ -Type Ag O Nano Composite for Visible Light Photocatalytic Degradation of Organic Dye ", The Journal of Physical Chemistry C, 2016 <1%
Publication

Xuefang Wang, Fengling Xia, Xichuan Li,

| | | |
|---|---|---|
| 48 | Xiaoyang Xu, Huan Wang, Nian Yang, Jianping Gao. "Fabrication of Bi-Fe3O4@RGO hybrids and their catalytic performance for the reduction of 4-nitrophenol", Journal of Nanoparticle Research, 2015<br>Publication | <1% |
| 49 | d-nb.info<br>Internet Source | <1% |
| 50 | Cheng Du, Shuijian He, Xiaohui Gao, Wei Chen. " Hierarchical Cu@MnO Core-shell Nanowires: A Nonprecious-Metal Catalyst with an Excellent Catalytic Activity Toward the Reduction of 4-Nitrophenol ", ChemCatChem, 2016<br>Publication | <1% |
| 51 | Mahmoud Nasrollahzadeh, Ebrahim Mehdipour, Mahboobe Maryami. "Efficient catalytic reduction of nitroarenes and organic dyes in water by synthesized Ag/diatomite nanocomposite using Alocasia macrorrhiza leaf extract", Journal of Materials Science: Materials in Electronics, 2018<br>Publication | <1% |
| 52 | Cheng Yang, Yan Yu, Yujun Xie, Dai Zhang, Pan Zeng, Yurong Dong, Bilin Yang, Rongqing Liang, Qiongrong Ou, Shuyu Zhang. "One-step synthesis of size-tunable gold nanoparticles/reduced graphene oxide | <1% |

nanocomposites using argon plasma and their applications in sensing and catalysis", Applied Surface Science, 2019
Publication

---

53 Zhang, Zhenyi, Changlu Shao, Yangyang Sun, Jingbo Mu, Mingyi Zhang, Peng Zhang, Zengcai Guo, Pingping Liang, Changhua Wang, and Yichun Liu. "Tubular nanocomposite catalysts based on size-controlled and highly dispersed silver nanoparticles assembled on electrospun silica nanotubes for catalytic reduction of 4-nitrophenol", Journal of Materials Chemistry, 2012.
Publication

<1%

---

54 Submitted to Indian Institute of Technology, Madras
Student Paper

<1%

---

55 Ankush Halbe, Graeme Housser, Michael Gardner, Timothy Groves, Pradeep Haldar. "Evaluation of reactive sputtering of ZnS in Ar-O2 environment as a pathway to Zn(O, S) thin-films", 2013 IEEE 39th Photovoltaic Specialists Conference (PVSC), 2013
Publication

<1%

---

56 Peng Dai, Mingzai Wu, Tongtong Jiang, Haibo Hu, Xinxin Yu, Zhiman Bai. "Silver-loaded ZnO/ZnFe2O4 mesoporous hollow spheres with

<1%

enhanced photocatalytic activity for 2,4-dichlorophenol degradation under visible light irradiation", Materials Research Bulletin, 2018
Publication

---

57 Zongwei Mei, Ning Zhang, Shuxin Ouyang, Yuanjian Zhang, Tetsuya Kako, Jinhua Ye. " Photoassisted fabrication of zinc indium oxide/oxysulfide composite for enhanced photocatalytic H evolution under visible-light irradiation ", Science and Technology of Advanced Materials, 2016 <1%
Publication

---

58 Wi, Jae-Hyung, Tae Gun Kim, Jeong Won Kim, Woo-Jung Lee, Dae-Hyung Cho, Won Seok Han, and Yong-Duck Chung. "Photovoltaic Performance and Interface Behaviors of Cu(In,Ga)Se2 Solar Cells with a Sputtered-Zn(O,S) Buffer Layer by High Temperature Annealing", ACS Applied Materials & Interfaces <1%
Publication

---

59 Submitted to North Carolina State University <1%
Student Paper

---

60 Wang, Changhua, Xintong Zhang, Yongan Wei, Lina Kong, Feng Chang, Han Zheng, Liangzhuan Wu, Jinfang Zhi, and Yichun Liu. "Correlation between band alignment and enhanced photocatalysis: a case study with <1%

anatase/TiO2(B) nanotube heterojunction", Dalton Transactions, 2015.
Publication

| | | |
|---|---|---|
| 61 | Wu Yang, Dezhi Chen, Hongying Quan, Shaolin Wu, Xubiao Luo, Lin Guo. " Enhanced photocatalytic properties of ZnFe O -doped ZnIn S heterostructure under visible light irradiation ", RSC Advances, 2016<br>Publication | <1% |
| 62 | pubs_rsc.gg363.site<br>Internet Source | <1% |
| 63 | china.iopscience.iop.org<br>Internet Source | <1% |
| 64 | Ahn, W.Y.. "Photocatalytic reduction of 4-nitrophenol with arginine-modified titanium dioxide nanoparticles", Applied Catalysis B, Environmental, 20070618<br>Publication | <1% |
| 65 | Chang, Y.C.. "Catalytic reduction of 4-nitrophenol by magnetically recoverable Au nanocatalyst", Journal of Hazardous Materials, 20090615<br>Publication | <1% |
| 66 | livrepository.liverpool.ac.uk<br>Internet Source | <1% |
| 67 | Zhen-Wu Jiang, Shou-Shuai Gao, Si-Yu Wang, | |

Dong-Xiao Wang, Peng Gao, Qiang Sun, Zhi-Qiang Zhou, Wei Liu, Yun Sun, Yi Zhang. "Insight into band alignment of Zn(O,S)/CZTSe solar cell by simulation", Chinese Physics B, 2019
Publication

<1%

68 Submitted to Deakin University
Student Paper

<1%

69 Gaiping Li, Yuexiang Wang, Lanqun Mao. "Recent progress in highly efficient Ag-based visible-light photocatalysts", RSC Adv., 2014
Publication

<1%

70 A. Hultqvist, C. Platzer-Björkman, E. Coronel, M. Edoff. "Experimental investigation of Cu(In1−x,Gax)Se2/Zn(O1−z,Sz) solar cell performance", Solar Energy Materials and Solar Cells, 2011
Publication

<1%

71 Junlei Zhang, Huan Liu, Zhen Ma. "Flower-like Ag 2 O/Bi 2 MoO 6 p-n heterojunction with enhanced photocatalytic activity under visible light irradiation", Journal of Molecular Catalysis A: Chemical, 2016
Publication

<1%

72 Wei Liu, Yu Fan, Xiaodong Li, Shuping Lin, Yang Liu, Sihan Shi, He Wang, Zhiqiang Zhou, Yi Zhang, Yun Sun. " Artificial twin-layer

<1%

configurations of Zn(O,S) films by radio frequency sputtering in all dry processed eco-friendly Cu(In,Ga)Se solar cells ", Journal of Physics D: Applied Physics, 2018
Publication

---

73 worldwidescience.org <1%
Internet Source

---

74 Submitted to University of Bahrain <1%
Student Paper

---

75 Chen, Long, Wei Ma, Jiangdong Dai, Juan Zhao, Chunxiang Li, and Yongsheng Yan. "Facile synthesis of highly efficient graphitic-C3N4/ZnFe2O4 heterostructures enhanced visible-light photocatalysis for spiramycin degradation", Journal of Photochemistry and Photobiology A Chemistry, 2016. <1%
Publication

---

76 Hairus Abdullah, Dong-Hau Kuo. " Photocatalytic Performance of Ag and CuBiS Nanoparticle-Coated SiO @TiO Composite Sphere under Visible and Ultraviolet Light Irradiation for Azo Dye Degradation with the Assistance of Numerous Nano p–n Diodes ", The Journal of Physical Chemistry C, 2015 <1%
Publication

---

77 Haifeng Wang, Lin Quan, Bo Hu, Guohui Wei, Xingmao Jiang. "Aerosol method assisted <1%

fabrication Ag@SiO2 and efficient catalytic activity for reduction of 4-nitrophenol", Micro & Nano Letters, 2017
Publication

---

78 Kong, L.. "Rattle-type Au@TiO"2 hollow microspheres with multiple nanocores and porous shells and their structurally enhanced catalysis", Materials Chemistry and Physics, 20101001 <1%
Publication

---

79 Submitted to University of New South Wales <1%
Student Paper

---

80 Huizhi Sun, Osman Ahmed Zelekew, Xiaoyun Chen, Yuanbo Guo, Dong-Hau Kuo, Qingxin Lu, Jinguo Lin. " A noble bimetal oxysulfide Cu OS catalyst for highly efficient catalytic reduction of 4-nitrophenol and organic dyes ", RSC Advances, 2019 <1%
Publication

---

81 Margi Jani, Dhyey Raval, Ranjan Kumar Pati, Indrajit Mukhopadhyay, Abhijit Ray. "Effect of annealing atmosphere on microstructure, optical and electronic properties of spray-pyrolysed In-doped Zn(O,S) thin films", Bulletin of Materials Science, 2018 <1%
Publication

---

82 Di Xu, Peng Diao, Tao Jin, Qingyong Wu,

| | | |
|---|---|---|
| | Xiaofang Liu, Xin Guo, Hongyu Gong, Fan Li, Min Xiang, Yu Ronghai. "Iridium Oxide Nanoparticles and Iridium/Iridium Oxide Nanocomposites: Photochemical Fabrication and Application in Catalytic Reduction of 4-Nitrophenol", ACS Applied Materials & Interfaces, 2015<br>Publication | <1% |
| 83 | Jinmin Zheng, Yalei Dong, Weifeng Wang, Yanhua Ma, Jing Hu, Xiaojiao Chen, Xingguo Chen. "In situ loading of gold nanoparticles on Fe3O4@SiO2 magnetic nanocomposites and their high catalytic activity", Nanoscale, 2013<br>Publication | <1% |
| 84 | Submitted to Heriot-Watt University<br>Student Paper | <1% |
| 85 | Submitted to University of Keele<br>Student Paper | <1% |
| 86 | Rufino M. Navarro Yerga, M. Consuelo Álvarez Galván, F. del Valle, José A. Villoria de la Mano, José L. G. Fierro. "Water Splitting on Semiconductor Catalysts under Visible-Light Irradiation", ChemSusChem, 2009<br>Publication | <1% |
| 87 | Dong-Hau Kuo, Roger Lo, Tien Hsiang Hsueh, Der-Jun Jan, Chi-Hung Su. "LiSnOS/gel polymer hybrid electrolyte for the safer and | <1% |

performance-enhanced solid-state LiCoO2/Li lithium-ion battery", Journal of Power Sources, 2019
Publication

| | | |
|---|---|---|
| 88 | Submitted to West De Pere High School<br>Student Paper | <1% |
| 89 | Helen Hejin Park, Rachel Heasley, Roy G. Gordon. "Atomic layer deposition of Zn(O,S) thin films with tunable electrical properties by oxygen annealing", Applied Physics Letters, 2013<br>Publication | <1% |
| 90 | Sahiner, Nurettin, and Selin Sagbas. "The preparation of poly(vinyl phosphonic acid) hydrogels as new functional materials for in situ metal nanoparticle preparation", Colloids and Surfaces A Physicochemical and Engineering Aspects, 2013.<br>Publication | <1% |

| | | | |
|---|---|---|---|
| Exclude quotes | Off | Exclude matches | Off |
| Exclude bibliography | On | | |